Planck-HFI optical design and pre-flight performances

B. Maffei*, F. Noviello†, G. Savini‡, J.A. Murphy§, J-M. Lamarre¶, P.A.R. Ade‖, F.R. Bouchet**, J. Brossard††
A. Catalano¶[xvi], R. Colgan§, R. Gispert†, E. Gleeson§, C.V. Haynes*, W.C. Jones‡‡[x], A.E. Lange[x], Y. Longval†
I. McAuley§, H.U. Nørgaard-Nielsen[xi], F. Pajot†, T. Peacocke§, G. Pisano*, J-L. Puget†, I. Ristorcelli[xii]
R. Sudiwala‖, J. Tauber[xiii], R.J. Wylde[xiv] and V. Yurchenko§[xv]

*JBCA, School of Physics and Astronomy, The University of Manchester, Oxford Road, Manchester M13 9PL, UK
Bruno.maffei@manchester.ac.uk

†Institut d'Astrophysique Spatiale, CNRS & Université Paris 11, Bâtiment 121, 91405 Orsay, France

‡Optical Science Laboratory, Dept. of Physics and Astronomy, UCL, London, WC1E 6BT, UK

§NUI Maynooth, Department of Experimental Physics, Maynooth, Co. Kildare, Ireland

¶LERMA, CNRS, Observatoire de Paris, 61 Avenue de l'Observatoire, 75014 Paris, France

‖Cardiff University, School of Physics and Astronomy, The Parade, Cardiff CF24 3AA, UK

**Institut d'Astrophysique de Paris, CNRS & Université Paris 6, 98bis Bd Arago, 75014 Paris, France

††Laboratoire de l'Accélérateur Linéaire, CNRS & Université Paris 11, Bâtiment 200, 91898 Orsay, France

‡‡Princeton University, Dept. of Physics, Princeton, NJ 08544, USA

[x]Caltech/JPL, Caltech Observational Cosmology, Mail code:59-33, Pasadena, CA 91125, USA

[xi]Danish National Space Center, Juliane Mariesvej 28, DK-2100, Copenhagen, Denmark

[xii]CESR, CNRS-Université, 9 av. du colonel Roche, BP44346, 31038 Toulouse Cedex 4, France

[xiii]European Space Agency (ESA), Astrophysics Division, Keplerlaan 1, 2201AZ Noordwijk, The Netherlands

[xiv]School of Physics and Astronomy, North Haugh, St Andrews, Fife KY16 9SS, UK

[xv]Institute of Radiophysics and Electronics, NAS of Ukraine, 12 Proskura St., 61085, Kharkov, Ukraine

[xvi]Laboratoire Astroparticule et Cosmologie, UMR 7164, Universit Paris Diderot - Paris, France

***Abstract*—Planck is a European Space Agency (ESA) satellite, launched in May 2009, which is mapping the Cosmic Microwave Background anisotropies in intensity and polarisation with unprecedented detail and sensitivity. It will also provide full-sky maps of astrophysical foregrounds. An accurate knowledge of the telescope beam patterns is an essential element for a correct analysis of the acquired astrophysical data. We present the optical design of the High Frequency Instrument (HFI) together with the optical performances measured during the ground calibration campaigns. We report on the evolution of the knowledge of the pre-launch HFI beam patterns when coupled to the telescope, and on their significance for the HFI data analysis procedure.**

I. Introduction

The ESA space mission Planck launched in May 2009 will finish its first full sky-survey in March 2010. Its goal is to map the whole sky at least three times in nine frequency bands comprised between 30 GHz and 1 THz. The primary objective of the Planck mission [1] is to measure the intensity and the polarisation of the temperature fluctuations of the Cosmic Microwave Background (CMB). In addition, because of its extended frequency coverage, Planck will improve our understanding of foreground emissions from both Galactic and extragalactic sources.

The Planck payload is equipped with two focal plane instruments, the Low Frequency Instrument (LFI) operating in three frequency bands at 30, 44 and 70 GHz [2], and the High Frequency Instrument (HFI) operating in six higher frequency bands [3]. The detectors of these two instruments are optically coupled to an off-axis dual-mirror telescope [4] satisfying the Mizuguchi-Dragone condition, which allows the system to operate without significant degradation in a large focal plane array, while simultaneously giving a very low level of cross-polarisation ([5], [6]). The primary mirror has a projected diameter of 1.5 m allowing a resolution ranging from 4.5 to 30 arcmin which results from an under-illumination of the primary reflector that minimises the spillover. HFI uses the central part of the focal plane to minimise aberrations at high frequency with LFI being located around it. While the two instruments are based on different detector technology, both make use of cold feed-horn cold antennas to focalise the incoming radiation from the telescope onto the detectors. The horn phase centres are distributed across the focal plane surface without any components in the path between the front horns and the telescope to avoid unwanted beam distortion, and care has been taken to avoid shadowing between and within the two instruments in order to avoid any diffractive effect that will impact the cleanliness of the beams. This resulted in another constraint while designing the cold optics in addition to the usual requirements in term of mass, dimensions, thermal properties and amongst all optical quality. Since the observed signal arriving from an astronomical source (such as the CMB) will be convolved with the beam response of the observing instrument, it is of paramount importance to acquire the best possible knowledge of the instrument.

II. The High Frequency Instrument

The HFI is a multi-frequency photometer comprising six spectral bands centred at 100, 143, 217, 353, 545 and 857GHz. The four lowest frequency bands are single-moded and a number of these channels have dual-polarisation capabilities using Polarisation Sensitive Bolometers (PSB), while the remaining single-mode channels, together with the two high frequency bands (multi-moded) are without polarisation determination (total power using Spider Web bolometers). The Planck-HFI detection system is based on highly sensitive bolometers cooled at 0.1 K which are photon noise limited. In order to get the best optical performances of these detectors, a specific detection assembly (Sec. II-B) has been designed allowing not only the optical specifications to be met but also to reach the mechanical and thermal requirements. Operating bolometers at such a low temperature makes the cryogenic chain complicated. Only an optimised thermal design can stop unwanted radiation from reaching the coldest stage and increasing the radiation background on the detectors. For this purpose, the thermal architecture relies on several enclosed thermal stages (similar to a Russian doll structure) each radiatively shielding the following one (Fig. 1). Starting from a common LFI-HFI 20K stage cooled by a closed cycle Hydrogen Joule-Thomson (J-T) cryocooler, another mechanical cryocooler based on Helium J-T expansion is providing a 4K stage on which HFI is anchored. From then the dilution system is operated providing two other thermal stages at 1.6K and 100mK. Each HFI channel is distributed over the 4K, 1.6K and 100mK stages to form a detection assembly.

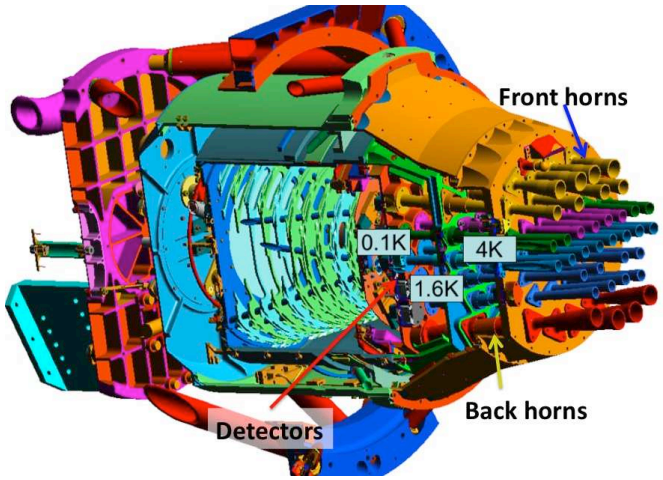

Fig. 1. HFI Focal Plane Unit.

A. Scientific requirements and instrument specifications

The scientific goals dictate the instrument requirements which, taking into account some trade-offs due to the mass restrictions, and telescope maximum diameter, lead to the instrument specifications. In order to reach the required sensitivity and the wide frequency coverage allowing a proper foreground separation, the HFI comprises:

- 4 pixels (or detection assemblies) for each of the polarised spectral bands (100, 143, 217 and 353 GHz)
- 4 pixels for each of the non-polarised (total intensity) spectral bands (143, 217 and 353 GHz)
- 4 pixels for each of the multi-mode channel (545 and 857 GHz)

Together with table I, the list of requirements is:

1) Spillover and straylight: These are important parameters to keep under control as they will result in an unwanted signal not directly originating from the source of interest. For a given telescope diameter we then need to have a trade-off between maximum resolution and spillover reduction.

2) Optical efficiency: Due to the detection assembly arrangement, the maximum theoretical optical efficiency (including the detector) cannot be higher than 60%. A requirement of 25% was set with a goal of 30%.

3) Focal plane curvature: The focal plane formed by the two instruments is relatively large and a specific optimisation took place [7] resulting in an aplanatic configuration with a curved focal surface. Each front horn phase centre had to be located on this focal surface.

Band Central freq.	Target Resolution	Spillover (%)	Edge Taper (dB)
100 GHz	9.2 arcmin	1 (0.5)	-25 (-30) at 25 deg
143 GHz	7.1 arcmin	0.7 (0.5)	-28 (-30) at 27 deg
217 GHz	5 arcmin	0.5 (0.3)	-30 (-32) at 26 deg
353 GHz	5 arcmin	0.5 (0.3)	-30 (-32) at 26 deg
545 GHz	5 arcmin	0.5 (0.3)	-30 (-32) at 26 deg
857 GHz	5 arcmin	0.5 (0.3)	-30 (-32) at 27 deg

TABLE I
SUMMARY OF OPTICAL REQUIREMENTS FOR EACH SPECTRAL BAND. NUMBERS IN PARENTHESES REFER TO THE GOAL WE WERE AIMING AT.

B. Optical concept

The optical requirements cannot be met by the use of smooth walled horns, therefore corrugated horns have been adopted. These have very low return and insertion losses, a low cross-polarisation level and a good directivity, making them the ideal components to couple the radiation to the detector. Their use reduces the spillover and allows for an efficient straylight control, giving a well-behaved beam shape definition. To further improve the sidelobe rejection, new profiled-flared horns have been developed [8]. Quasi-optical components (dewar window and filters) located in front of the horn aperture will affect the horn beam shape [9]. In order to take advantage of the fact that Planck is in space where no dewar window is needed, an important issue is to determine the optimum position at which to put the interference spectral filters needed for the bolometers. Based on a design put forward for a previous experiment [10], we make use of a triple horn configuration defining a detection assembly (Fig. 2). The radiation from the telescope is focussed onto the entrance of a back-to-back horn pair. A lens located in between the back horn and the detector horn, in conjunction of the profiled geometry of both horns, creates a beamwaist where wavelength selective filters can be placed, and allows

the radiation to be properly coupled to the bolometric detector. Another significant benefit of this arrangement is that the various components can be placed on different temperature stages to create thermal breaks and thus reduce the level of background power onto the bolometer and cooling system [11].

The bolometric detectors developed by Caltech/JPL are of two kinds. Spider web NTD Germanium bolometers (SWB) [12] to detect the total radiation intensity and Polarisation Sensitive Bolometer (PSB) [13] technology to be able to detect two orthogonal polarisation orientation within the same device.

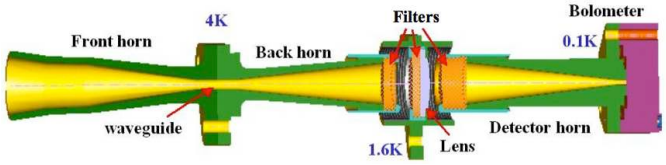

Fig. 2. HFI detection assembly chain. The back-to-back horn (front and back horns) couples the incoming radiation from the telescope to a detector horn which then couples the radiation to the bolometric detector. Filters are located in between the two horn assemblies in order to define the spectral band. A lens refocusses the radiation from the back horn to the detector horn.

III. Optical design and performances

A. Front horn beam definition

For the single-mode channels, the corrugated waveguide of the back-to-back horn pair is designed to filter out all but the TE_{11} and TM_{11} modes resulting in a single fundamental hybrid mode HE_{11}, combination of the TE_{11} and TM_{11} scattering matrix modes. The waveguide also defines the high frequency pass cut-on of the spectral band, frequency below which no mode can be transmitted.

While a diffraction limited projected aperture of 1.5m could in principle give an angular resolution of a few arcminutes for frequencies above 300 GHz ([3], [1]) a maximum resolution of 5 arcminutes was required. We have chosen to slightly under-illuminate the telescope for the 353 GHz band while the 545 and 857 GHz bands are multi-mode channels [14] for which the back-to-back horn waveguides have been designed to allow a larger number of higher order modes above the TE_{11} or the TM_{11} modes to propagate. The latter technique has the advantage of increasing the sensitivity of the detection assembly, each mode bringing its contribution to the power detected, but has the drawback of resulting in a beam which is more complicated to model and less predictable than single-mode channels.

Software based on modal matching techniques have been used to compute the beam patterns of the profiled-flared horn geometries [8]. An example of such beam patterns compared with the experimental beam profile measured on one of the flight model horns (100 GHz) is given in fig. 4.

B. Optical efficiency optimisation

The sensitivity of the instrument is strongly dependant on the overall optical efficiency that can be achieved. The optical

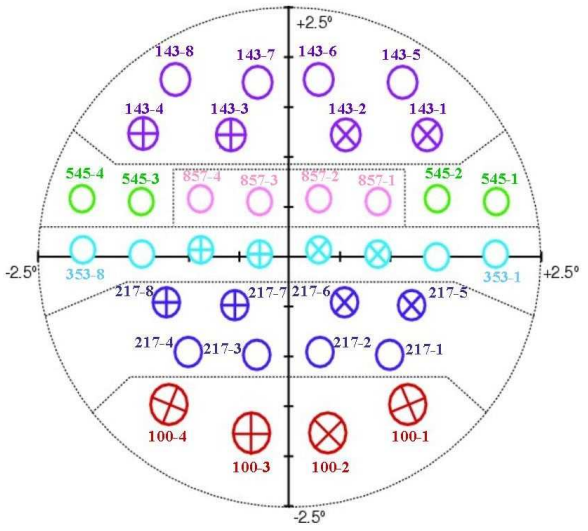

Fig. 3. HFI focal plane layout. Empty circles represent the location of the front horn of each total intensity pixel. The crosses within the circles give the axis orientation of the dual-polarised detectors a and b of the PSBs.

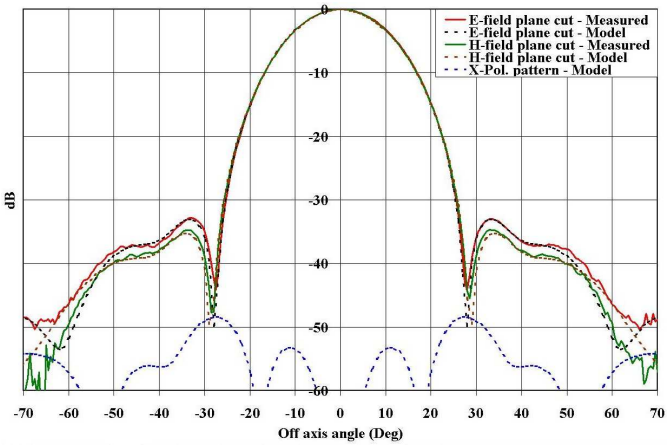

Fig. 4. Typical back-to-back horn beam pattern at 100 GHz. The 2 co-polarisation beams (model and experimental data) are shown (E and H planes) as well as the model of the cross-polarisation beam.

coupling between the various components of the detection assemblies is the major parameter affecting the optical efficiency. Special attention has been adopted in optimising each section of the detection assemblies while keeping the instrumental cross-polarisation to a minimum. The optical couplings between the back horn and the detector horn through the lens and interference filters, as well as between the detector horn and the SWB and PSB detectors have been simulated and optimised with the finite element analysis software HFSS (www.ansoft.com). While a more detailed description of the approach and analysis is given in ref. [15], measured results during the calibration campaigns on the Focal Plane Unit (FPU) flight model are given in table II. A more accurate analysis of the multi-mode channels (future publication), taking into account the measured spectral bands should lead to a higher optical efficiency.

IV. Focal plane unit performances

A. Spectral performances

The spectral selection of incoming radiation is obtained in pixels of each channel by a combination of waveguide extinction at lower frequencies and metal-mesh filters embedded in polypropylene substrates.

In the single-mode channels, the low frequency side of the band cut-on is determined by the waveguide section of the back-to-back corrugated horn pair. The filters which are all positioned between the 3 thermal stages (fig. 2) in the coupling stage are tuned in order to progressively reject radiation at higher frequencies. The single cut-off frequency of each filter is chosen as to exclude any small resonance peak that might occur from the previous filter. In the multi-mode channels (545 and 857 GHz) low frequency rejection is further obtained by adopting a high-pass metal mesh filter [11]. All spectral bands are designed to have a 33% relative bandwidth and to be contiguous in order to cover smoothly all the spectrum from 85GHz to 1 THz.

Calibration of the spectral bands and their detailed shape cannot be refined in flight and so required detailed measurements in ground facilities. Due to the noise floor of the measurements in the Saturne ground based calibration facility [16], the final spectral transmissions of the HFI channels (fig. 5) were obtained by combining the calibration test data for the in-band region, with the instrument focal plane assembled as in flight, with out-of-band data obtained conservatively by assuming close to unit efficiency of other optical components and simply multiplying the single filter profiles measured separately. With this compromise it is possible to verify the required out-of-band rejection criteria to be satisfied (10^{-15} at wavenumbers greater than 200 cm^{-1} for the highest frequency channel).

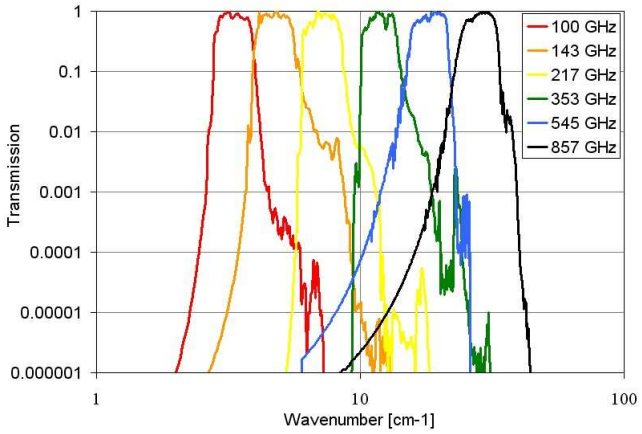

Fig. 5. Measurement results of the six HFI spectral bands.

V. Antenna beam prediction

Accurate measurements of the beam characteristics on the ground require the use of compact test ranges (CATR), but cannot be performed in exact flight-like conditions. A set of such measurements were taken in a system-level validation campaign at 30, 70, 100 and 320 GHz ([4], [17]). For this reason the pre-launch beam knowledge relies on accurate simulations.

The antenna beam patterns of the horns at the operating temperature of 4K were computed with the commercial CORRUG (S.M.T. Consultancies Ltd) and the NUI Maynooth SCATTER software packages. These patterns were then propagated through the telescope optics with the TICRA GRASP (versions 8 and 9) reflector antenna analysis software package [18]. In the following simulations, except when stated otherwise, we consider an ideal telescope (a telescope model with design alignments and smooth mirror theoretical surfaces). The telescope baffles were not included in these simulations since the radiation intercepted by them does not contribute to the main beam power pattern.

For the single-mode channels, the TE_{11} and TM_{11} were propagated separately through the telescope. The patterns resulting from both input modes will essentially exit the system as an HE_{11} (a mixture of TE_{11} and TM_{11} - although with different power contents). For the unpolarised HFI single-mode channels, the two orthogonal HE_{11} modal fields are

Channel Label	**100**	**143P**	**217P**	**353P**
Centre Freq. (GHz)	101.0	142.3	219.2	359.3
Centre Freq. Dispersion σ(GHz)	0.58	0.71	0.38	2.02
Upper band edge (GHz)	118	163	253	408
Lower band edge (GHz)	85	121	182	306
Av. filter transmission over 30% bandwidth	0.81	0.83	0.79	0.79
Bandwidth (GHz)	29.8	42.1	63.5	91.9
BW Dispersion σ(GHz)	1.4	1.4	1.0	7.1
Beam width (arcmin)	9.6	7.0	4.5/4.7	4.8
Ellipticity min/max	0.14	0.07/012	0.09/0.12	0.05/0.12
Av. optical eff. (%)	32.2	43.2	31.3	21.3

Channel Label	**143U**	**217U**	**353U**	**545**	**857**
Centre Freq. (GHz)	143.6	221.7	361.3	556.3	863.1
Centre Freq. Dispersion σ(GHz)	0.56	0.33	2.29	1.57	5.36
Upper band edge (GHz)	166	253	411	641	992
Lower band edge (GHz)	121	189	306	467	734
Av. filter transmission over 30% bandwidth	0.83	0.79	0.79	0.57	0.54
Bandwidth (GHz)	43.8	60.6	95.7	165.9	248.8
BW Dispersion σ(GHz)	0.4	1.6	4.4	3.1	8.1
Beam width (arcmin)	7.15	4.85	4.55	-	-
Ellipticity	0.06	0.13	0.15	-	-
Av. optical eff. (%)	28.7	25.7	23.4	15.7	13.1

TABLE II
TELESCOPE BEAM PERFORMANCES (FROM SIMULATIONS ASSUMING PERFECT OPTICAL COMPONENTS). THE MEASURED OPTICAL EFFICIENCIES RESULT FROM THE CALIBRATION CAMPAIGNS

Detection Assembly	**FWHM (Arcmin)**	**HPBW (Arcmin)**
545-2	4.85 x 4.69	3.74 x 3.36
857-1	5.05 x 4.84	3.67 x 3.45

TABLE III
FWHM AND HPBW ESTIMATED FOR TWO BROAD-BAND SIMULATIONS PERFORMED ON THE 545 GHZ AND 857 GHZ CHANNELS.

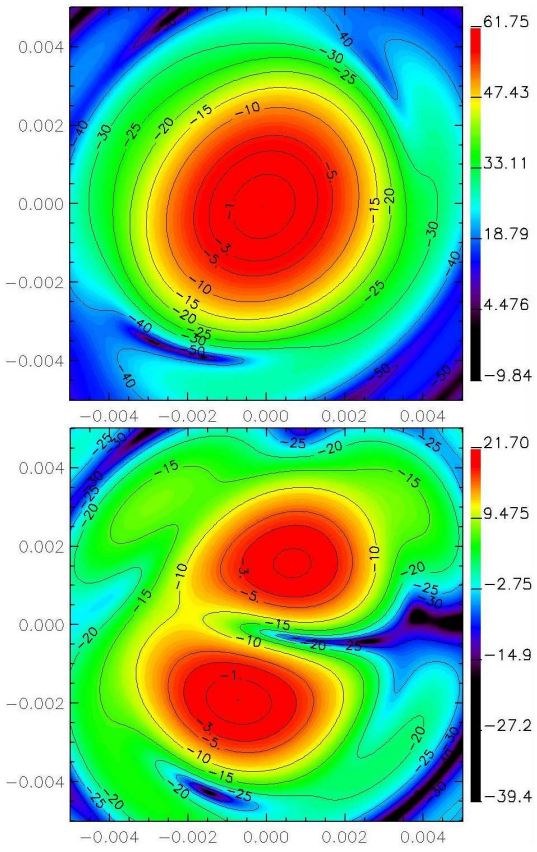

Fig. 6. Top: co-polarisation; Bottom: cross-polarisation main beam intensity maps for the polarised detector 100-2a. Simulations performed using ideal telescope and horns at the central frequency of 100 GHz. Color scale: gain. Contours in dB respectively to maximum. The peak cross-pol is about -40dB.

propagated independently through the telescope (since there is no phase relationship between them) and are then added in quadrature in the far-field. It is important to note that the cross-polarisation beams computed here do not take into account the cross-polarisation of the full detection assemblies which is dominated by the horn to PSB coupling as mentioned in the previous section (few % typically). In the beam simulation only the polarisation effects of perfect horns and mirrors (about -40 dB level) are taken into account. Table II summarises the performances of the HFI beams while fig. 6 is showing one of the main beam simulation results.

The quadrature sum approach is also used for multi-mode channels for which the fields are incoherent sums of all HE and EH modes of different orders that can propagate. The number of modes transmitted through the detection assemblies that reach the bolometer varies with frequency, giving a non-constant number of modes across each spectral band. Therefore the main beam structure will vary with frequency. Since the main beam will not be Gaussian, a classic Full Width Half Maximum (FWHM) used on a typical quasi-Gaussian main beam becomes an inappropriate measure of the beam width here. A better definition is the Half Power Beam Width (HPBW) as shown in Table III.

VI. Conclusions

We have described the design optimisation of the cold optics and of the focal plane unit of Planck-HFI. The measured optical performances of the resulting instrument flight model are presented, together with beam simulations based on the perfect optical system.

Some of the ground calibration data are still being analysed and the results will be combined with in-flight calibration in order to get a more accurate knowledge of the instrument. Further post-launch publications will then be available.

Acknowledgment

The authors would like to acknowledge the support from STFC, CNRS, CNES, ESA, NASA, Enterprise Ireland and Science Foundation Ireland.

References

[1] J. Tauber *et al.*, "Planck pre-launch status: the planck mission," *submitted to A&A*, 2010.
[2] M. Bersanelli *et al.*, "Planck pre-launch status: design and description of the low-frequency instrument," *submitted to A&A*, 2010.
[3] J. Lamarre *et al.*, "Planck pre-launch status: the HFI instrument, from specification to actual performance," *accepted in A&A*, 2010.
[4] J. Tauber *et al.*, "Planck pre-launch status: the optical system," *submitted to A&A*, 2010.
[5] Y. Mizuguchi, M. Akagawa, and H. Yokoi, "Offset Gregorian antenna," *Electronics Communications of Japan*, vol. 61, pp. 58–66, Mar. 1978.
[6] C. Dragone, "A first-order treatment of aberrations in Cassegrainian and Gregorian antennas," *IEEE Transactions on Antennas and Propagation*, vol. 30, pp. 331–339, May 1982.
[7] D. D. C. M. Fargant, G. *et al.*, "Very wide band telescope for Planck using optical and radio frequency techniques," in *Society of Photo-Optical Instrumentation Engineers (SPIE) Conference Series*, vol. 4013, 2000, p. 69.
[8] B. Maffei *et al.*, "Shaped corrugated horns for cosmic microwave background anisotropy measurements." *Int. J. Infrared and Millimetre waves*, vol. 21, p. 2023, 2000.
[9] B. Maffei *et al.*, "Effects of quasi-optical components on feed-horn co- and cross-polarisation radiation patterns," in *Society of Photo-Optical Instrumentation Engineers (SPIE) Conference Series*, vol. 7020, Aug. 2008.
[10] S. E. Church *et al.*, "A Compact High-Efficiency Feed Structure for Cosmic Microwave Background Astronomy at Millimetre Wavelengths," in *Submillimetre and Far-Infrared Space Instrumentation*, ser. ESA Special Publication, E. J. Rolfe & G. Pilbratt, Ed., vol. 388, Dec. 1996.
[11] P. Ade *et al.*, "Planck pre-launch status: the optical architecture of the HFI," *accepted in A&A*, 2010.
[12] W. Holmes *et al.*, "Initial test results on bolometers for the Planck high frequency instrument," *Appl Opt.*, vol. 47, pp. 5996–6008, Nov. 2008.
[13] W. C. Jones, R. Bhatia, J. J. Bock, and A. E. Lange, "A Polarization Sensitive Bolometric Receiver for Observations of the Cosmic Microwave Background," in *Society of Photo-Optical Instrumentation Engineers (SPIE) Conference Series*, T. G. Phillips & J. Zmuidzinas, Ed., vol. 4855, Feb. 2003, pp. 227–238.
[14] J. Murphy *et al.*, *submitted to Journal of Instrumentation*, 2010.
[15] B. Maffei *et al.*, "Planck pre-launch status: HFI polarization characteristics," *accepted in A&A*, 2010.
[16] F. Pajot *et al.*, "Planck pre-launch status: HFI ground calibration," *submitted to A&A*, 2010.
[17] M. Paquay *et al.*, "RCS Measurements at 320 GHz to Verify the Alignment of the PLANCK Reflector Configuration," in *EUROPEAN MICROWAVE CONFERENCE*, vol. 1-3, 2008, pp. 1273–1276.
[18] K. Pontoppidan, *GRASP9 Technical Description*. TICRA Engineering Consultants, 2005.